



## Short range stiffness elastic limit depends on joint velocity

Erwin de Vlugt<sup>a,\*</sup>, Stijn van Eesbeek<sup>a</sup>, Patricia Baines<sup>a</sup>, Joost Hilde<sup>a</sup>,  
Carel G.M. Meskers<sup>b</sup>, Jurriaan H. de Groot<sup>b</sup>

<sup>a</sup> Department of Biomechanical Engineering, Faculty of Mechanical Engineering, Laboratory for Neuromuscular Control, Delft University of Technology, Mekelweg 2, 2628 CD Delft, The Netherlands

<sup>b</sup> Department of Rehabilitation Medicine, Leiden University Medical Center, Laboratory for Kinematics and Neuromechanics, Albinusdreef 2, 2333 ZA Leiden, The Netherlands

### ARTICLE INFO

Article history:  
Accepted 17 May 2011

Keywords:  
Short range stiffness  
Joint stiffness  
Muscle  
Cross-bridges  
Elastic limit  
Model  
Identification

### ABSTRACT

Muscles behave as elastic springs during the initial strain phase, indicated as short range stiffness (SRS). Beyond a certain amount of strain the muscle demonstrates a more viscous behavior. The strain at which the muscle transits from elastic- to viscous-like behavior is called the elastic limit and is believed to be the result of breakage of cross-bridges between the contractile filaments. The aim of this study was to test whether the elastic limit, measured *in vivo* at the wrist joint, depended on the speed of lengthening. Brief extension rotations were imposed to the wrist joint ( $n=8$ ) at four different speeds and at three different levels of voluntary torque using a servo controlled electrical motor. Using a recently published identification scheme, we quantified the elastic limit from measured joint angle and torque. The results showed that the elastic limit significantly increased with speed in a linear way, indicating to a constant time of approximately 30 ms before cross-bridges break. The implications for movement control of the joint are discussed.

© 2011 Elsevier Ltd. All rights reserved.

### 1. Introduction

Muscles exhibit a relatively high stiffness over a short time interval just after an imposed length change, referred to as the short range stiffness, or SRS (Kirsch et al., 1994; Lin and Rymer, 1993; Morgan, 1977; Rack and Westbury, 1974; Walmsley and Proske, 1981). When lengthening or shortening continues, the stiffness drops and the muscle starts to act more like a viscous damper (Rack and Westbury, 1974). The length change or strain at which transition from high to low stiffness occurs is known as the elastic limit (Campbell and Lakie, 1998). For movement control, in particular the maintenance of body posture, regulation of joint stiffness is important for minimization of joint displacement in the presence of (external) disturbing forces. In particular, the response to the first part of an unexpected movement must largely be determined by the muscle properties since some time is required before any form of reflex response can develop (Grillner, 1972). In that respect it is important to determine the elastic limit under various loading conditions. The elastic limit has been studied extensively from single muscle fibers or muscles in animal preparations (Cui et al., 2007; Kirsch et al., 1994; Lin and Rymer, 1993; Morgan, 1977; Walmsley and Proske, 1981). From these studies it can be concluded that the elastic

limit increases with the velocity of lengthening (Campbell and Lakie, 1998). However, a systematic study on the effect of joint angular velocity on the elastic limit in humans is lacking. Past studies on the *in vivo* human joint that focused on SRS were limited to passive conditions and slow movements to avoid additional torque changes from stretch reflexes (Axelson and Hagbarth, 2001; Lakie et al., 1984; Loram et al., 2007). Using an identification procedure we were able to estimate SRS and its concomitant elastic limit *in vivo* at different levels of muscle activation and fast rotations (van Eesbeek et al., 2010).

The main goal of the present study was to test the dependency of SRS and the elastic limit on wrist joint rotation velocity and voluntary torque. The results are important for future studies on neuromuscular control and disorders of joint impedance.

### 2. Methods

Essential aspects of the used method for estimation of short range stiffness (SRS) are provided but for a full description of the method the reader is referred to a previous study (van Eesbeek et al., 2010).

#### 2.1. Instrumentation

Ramp-and-Hold (RaH) extension rotations were imposed to the wrist joint by an electric motor, controlled as a stiff (1000 N m/rad) servo. The wrist flexion-extension axis was aligned to the motor axis. The forearm was immobilized with respect to the hand using clamps at distal and proximal radius and ulna such that

\* Corresponding author.

E-mail address: [e.devlugt@tudelft.nl](mailto:e.devlugt@tudelft.nl) (E. de Vlugt).

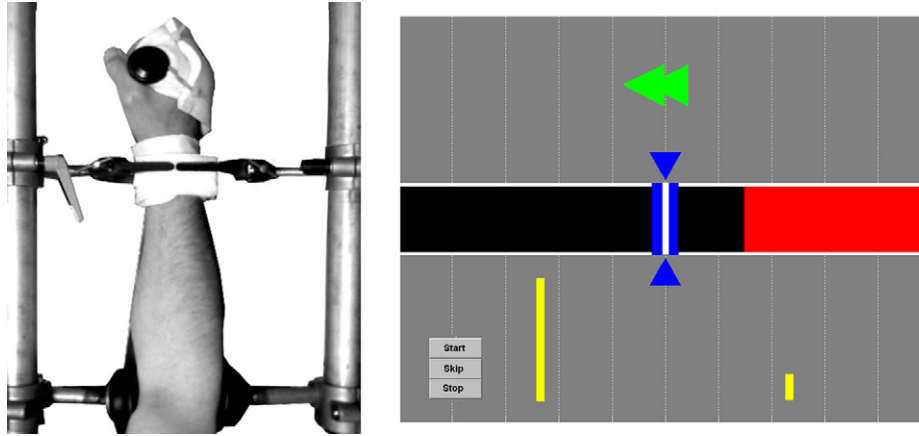


**Fig. 1.** Left: Experimental setup (top view). The elbow was fixed with stiff rubber clamps. The styloidei were fixed with PP foam malls and the hand was fixed to the manipulator handle with a PP foam mall and tie wraps. Right: display for visual feedback to the subject. Wrist flexion torque was visualized by a moving horizontal red bar that emerged from the right (right wrist of all subjects). Green arrows indicated the direction of torque to be applied. Target torque was indicated by the blue area ( $\pm 2.5\%$  of target torque level). Flexor and extensor muscle activity was displayed by vertical yellow bars (left and right respectively) of which the height was proportional to the EMG (normalized to MVC) of the corresponding muscles. EMG feedback was provided to minimize co-contraction. (For interpretation of the references to color in this figure legend, the reader is referred to the web version of this article.)

the rotation imposed by the motor resulted only in flexion/extension rotation of the wrist joint (Fig. 1). To fixate the hand to the motor handle, an individually fitted polypropylene PP foam mall was placed over the metacarpo-phalangeal joints using tie wraps. Angular displacement was measured by a digital encoder (Stegmann SRS50, Düsseldorf, Germany). Torque exerted onto the handle was measured by strain gauges within the handle lever. Activity of the flexor carpi radialis (FCR) and extensor carpi radialis (ECR) was recorded by EMG (Delsys Bagnoli-4, 20–450 Hz band-pass, 10 mm inter-electrode distance), full-wave rectified. All signals were sampled at 2.5 kHz and low-pass filtered (50 Hz, 3rd order recursive Butterworth).

2.2. Experimental protocol

Eight volunteers ( $25 \pm 4$  years, four male) participated in the study and signed an informed consent. Different combinations of four angular velocities (1.3, 1.95, 2.6 and 3.25 rad/s) and three target torques (0.9, 1.5 and 2.1 Nm) were applied in randomized order. Each combination was applied three times. The RaH started automatically when the difference between actual and target torque was smaller than 2.5% for at least 0.5 s. A 5 s rest period was included after each RaH movement. Visual feedback of the wrist torque was provided to the subject (Fig. 1). FCR and ECR EMG (low-pass filtered) were continuously displayed on the screen (Fig. 1) to assist the subjects in minimizing co-contraction. Subjects were also asked not to squeeze the handle. Total duration of the experiment was approximately 45 min.

2.3. Impedance model

For estimating the SRS, a dynamic nonlinear model was used, including all relevant compliant structures that were deformed by the imposed movement, i.e. those related to the lever, the handle–hand interface and the wrist joint (Fig. 2). The model was expressed in the angular (wrist joint) domain. No attempt was made to discriminate between individual contributions of muscles and tendons and load sharing between muscles was assumed constant. The model consisted of three pairs of spring-damper elements separated by two inertial loads;  $I_l$  is inertia of the lever plus handle and  $I_j$  the inertia of the wrist joint. Subsystem I includes the stiffness,  $k_l$ , and damping,  $b_l$ , of the lever compliance. Subsystem II includes the elasticity,  $k_h$ , and viscosity,  $b_h$ , of the handle–hand interface, e.g. from hand skin tissues. Subsystem III includes the elasticity,  $k_j$ , and viscosity,  $b_j$ , of the combined muscle–tendon units involved in the generation of the required joint torque. The spring,  $k_j$ , was designed as a nonlinear bi-phasic stiffness:

$$k_j = \begin{cases} k_{srs} & \theta_j < x_e \\ k_{srs} - k_{dec} & \theta_j > x_e \end{cases} \quad (1)$$

where  $k_{srs}$  is the joint SRS,  $x_e$  the elastic limit and  $k_{dec}$  the decrease in stiffness beyond  $x_e$  (Fig. 3) and implemented as a logarithmic torque–angle relationship:

$$T_{j,elas} = k_{srs} \theta_j - \log[1 + \exp(a_s \cdot k_{dec} \cdot (\theta_j - x_e))] / a_s \quad (2)$$

where  $T_{j,elas}$  is the elastic joint torque and  $a_s = 100$  a (fixed) smoothness parameter for the stiffness transition at  $x_e$ . Stiffness beyond the elastic limit was taken as  $k_{after} = k_{srs} - k_{dec}$ . Elapsed time,  $t$ , from onset of the RaH to the moment where the

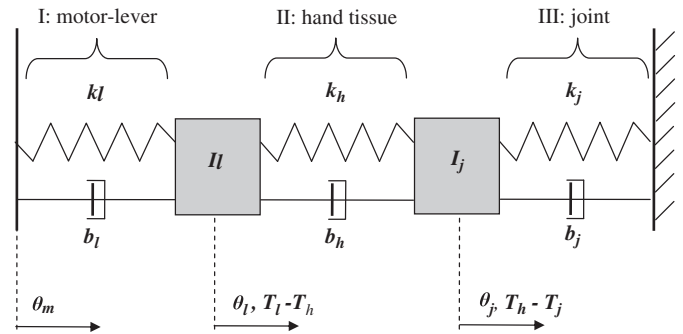


**Fig. 2.** Schematic presentation of the dynamic model used for parameter estimation. The model was expressed in the ‘angular’ domain and includes two inertial loads  $I_l$  and  $I_j$ , representing the inertia of the lever plus handle and the human wrist joint, respectively. The inertias were separated by three visco-elastic compartments, being: I, the motor lever (indexed by  $l$ ); II, the hand tissues (indexed by  $h$ ); III, the joint (indexed by  $j$ ). Viscous elements are indicated by  $b$ , stiffness elements by  $k$ , angles by  $\theta_m$ ,  $\theta_l$  and  $\theta_j$  for the motor axis, lever handle and wrist joint, respectively and torque by  $T_l$ ,  $T_h$  and  $T_j$  for the lever, hand and the joint, respectively.  $T_l$  and  $\theta_m$  were available from recordings.

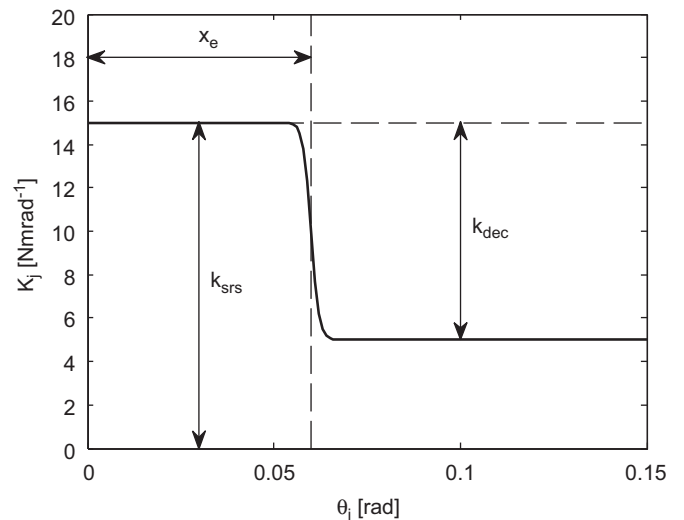


**Fig. 3.** Stiffness profile of the nonlinear spring as used to describe the joint stiffness:  $x_e$  represents the elastic limit, marking the angle of stiffness transition  $k_{dec}$  from the short range stiffness  $k_{srs}$  to the stiffness beyond the elastic limit.

**Table 1**  
Model parameters.

Parameter	Description	Unit	Parameterization
$I_l$	Manipulator Lever inertia	kg m <sup>2</sup>	Fixed
$b_l$	Manipulator Lever damping	N ms/rad	Fixed
$k_l$	Manipulator Lever stiffness	N m/rad	Fixed
$b_j$	Joint damping	N m s/rad	Fixed
$I_j$	Joint inertia	kg m <sup>2</sup>	Optimized
$b_h$	Hand–handle interface damping	N m s/rad	Optimized
$k_h$	Hand–handle interface stiffness	Nm/rad	Optimized
$k_{srs}$	Short range stiffness (SRS)	N m/rad	Optimized
$k_{dec}$	Stiffness beyond elastic limit (decrement to $k_{srs}$ )	N m/rad	Optimized
$x_e$	Elastic limit	rad	Optimized
$k_{after}$	Stiffness beyond the elastic limit	N m/rad	$k_{srs} - k_{dec}$
$x_t$	SRS period	s	From $x_e$ (see Section 2)

(simulated) joint angle was equal to the elastic limit was called the “SRS period”. The complete model is expressed by the following set of differential equations:

$$I_l \ddot{\theta}_l = T_l - T_h \quad (3)$$

$$I_j \ddot{\theta}_j = T_h - T_j \quad (4)$$

where  $T_l$  is the torque within the lever,  $T_h$  the torque from the hand–handle interface and  $T_j$  the joint torque:

$$T_l = b_l(\dot{\theta}_m - \dot{\theta}_l) + k_l(\theta_m - \theta_l) \quad (5)$$

$$T_h = b_h(\dot{\theta}_l - \dot{\theta}_j) + k_h(\theta_l - \theta_j) \quad (6)$$

$$T_j = b_j \dot{\theta}_j + T_{j,elas} \quad (7)$$

The parameters are listed in Table 1.

#### 2.4. Data analysis

The model parameters were estimated by minimization of the quadratic difference between the measured and predicted torque  $T_l$ . Torque and angle just before the start of the RaH movement ( $t=t_0$ ) were defined as  $\theta_0$  and  $T_0$ , respectively and were subtracted from the corresponding RaH traces because the model only described changes with respect to steady state behavior. To eliminate variation in muscle activity from stretch reflexes, parameterization was exclusively performed on the signals measured within 40 ms after the start of the RaH. The model was implemented in Simulink and the optimization was performed in Matlab (The Mathworks Inc.) using a nonlinear gradient search algorithm.

Model parameters for lever inertia, stiffness and damping ( $I_l$ ,  $k_l$ ,  $b_l$ ) were taken from (van Eesbeek et al., 2010) and kept constant throughout all optimizations. Joint damping,  $b_j$ , appeared to have a negligible effect on the predicted torque,  $\hat{T}_l$ , and was therefore fixed at a small value ( $10^{-5}$  Nm s/rad) to provide for numerical stability. For each subject a total of six parameters ( $b_h$ ,  $k_h$ ,  $I_j$ ,  $k_{srs}$ ,  $k_{dec}$ ,  $x_e$ ) remained to be estimated. The model parameters were optimized for all conditions (angular velocities, torque levels) simultaneously and this procedure was repeated for all repetitions. During the optimization, model parameters were free for each condition, except for the hand inertia  $I_j$ , which was taken equal for all conditions. Integrity of the model fit was indicated by the variance accounted for (VAF)

$$VAF = 1 - \frac{\sum_{i=1}^n (\theta_{m,i} - \hat{\theta}_{m,i})^2}{\sum_{i=1}^n (\theta_{m,i})^2} \quad (8)$$

where  $i$  indexes the time sample,  $n=100$  the number of data points,  $\theta_{m,i}$  the measured and  $\hat{\theta}_{m,i}$  the modeled motor angle. Parameter reliability was indicated by the Standard error of the mean (SEM)

$$SEM = \sqrt{\frac{1}{n} \cdot I \cdot (J^T \cdot J)^{-1} \sum_{i=1}^n (E_i)^2} \quad (9)$$

with  $E_i = T_{li} - \hat{T}_{li}$  the error of fit,  $J$  is the Jacobian ( $n \times n_p$ ) vector of first derivatives of the error to each parameter, with  $n_p=6$  the number of parameters, and  $I$  the identity matrix. Eq. (9) produces a vector of  $n_p$  SEM values for each optimized model parameter. The SEM equals the deviation of the parameter to its theoretical value at the minimal (optimal) error. SEM was normalized to the corresponding parameter value. A General Linear Model repeated measurements ANOVA was used to test the effect of movement velocity and torque (as within subjects variables) on the estimated parameters using SPSS 16.0 (SPSS Inc.) at an alpha of 0.05.

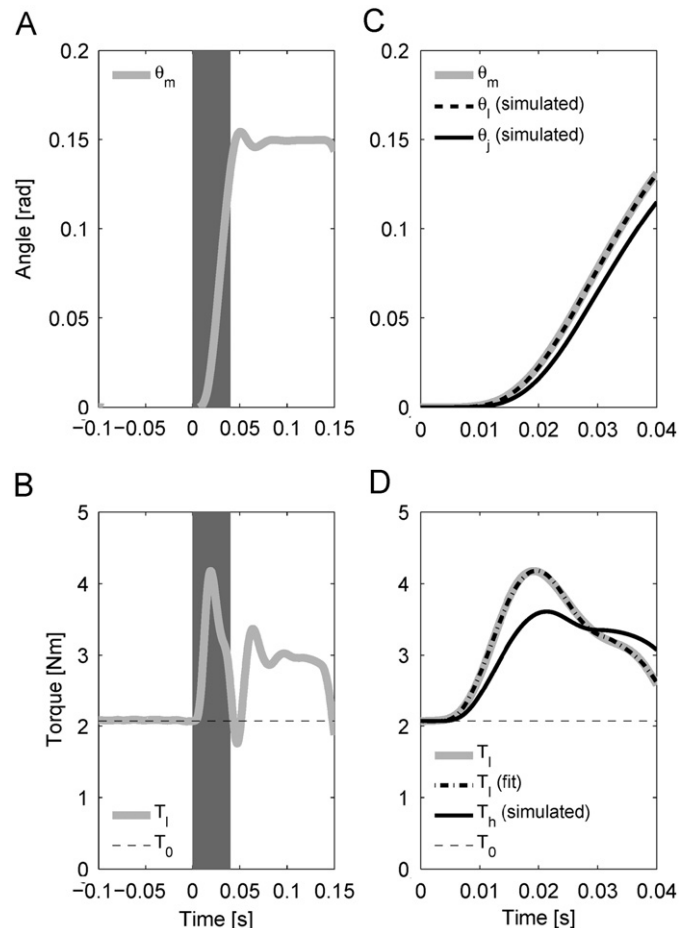


**Fig. 4.** Example of a data recording (A, B) and a typical model fit (C, D) for a subject ( $T_0=2.1$  Nm, 3.25 rad/s) at expanded time axes. A: measured angle  $\theta_m$ . B: measured torque  $T_l$ . Gray shaded areas in A and B denote the 40 ms time window used for parameterization of the model. C:  $\theta_m$  together with the simulated lever angle  $\theta_l$  and simulated joint angle  $\theta_j$ . D:  $T_l$  and fitted version together with the simulated hand torque  $T_h$ . For purpose of displaying,  $T_0$  (dashed lines) was added to the torque traces in B and D.

### 3. Results

#### 3.1. Model fit

Fig. 4 shows typical recordings of motor angle and lever torque (Fig. 4A and B). Gray shaded areas indicate the 40 ms time frame used for the parameter estimation. Fig. 4C shows the simulated lever and joint angles. The recorded and fitted lever torque are

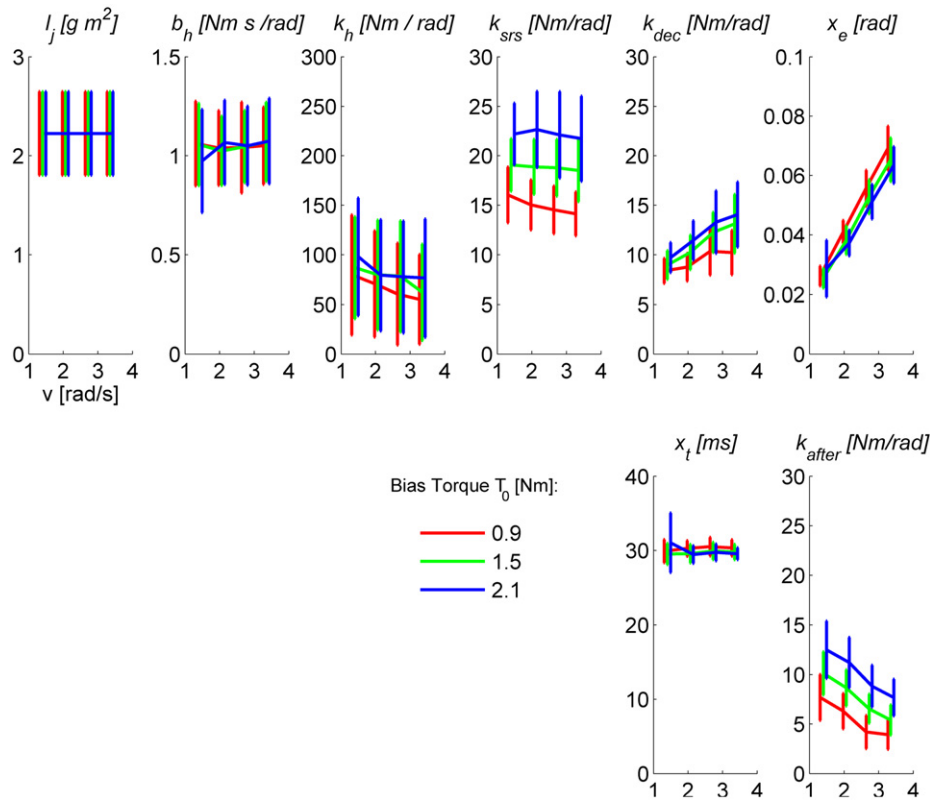


**Fig. 5.** Estimated model parameters (top row) averaged over all subjects and observations (mean  $\pm$  1 s. d. ) for the three incremented torque levels (red, green and blue) and movement velocities (horizontal axes). The SRS period,  $x_t$  (bottom row), was derived from the estimated parameters and the model simulation and taken as the elapsed time from the onset of the RaH to the time instance where the (simulated) joint angle was equal to the elastic limit. The stiffness beyond the elastic limit,  $k_{after}$  (bottom row), was taken equal to  $k_{srs} - k_{dec}$ . (For interpretation of the references to color in this figure legend, the reader is referred to the web version of this article.)

shown in Fig. 4D. For all subjects and conditions, the model was able to accurately describe the recorded torque, indicated by high VAF values of  $0.994 \pm 0.001$ . SEM values were smaller than 0.1 on average, meaning that all parameters were estimated within 10% from the optimal 'theoretical' value. To test for possible suboptimal solutions (local minima) we performed the optimization for different initial parameter values but never found noticeable differences in the estimated parameters.

### 3.2. Effect of angular velocity on SRS

Fig. 5 shows all estimated model parameters against velocity and for all torque levels, averaged over subjects and observations. Hand tissue elasticity,  $k_h$ , slightly decreased with velocity ( $p=0.002$ ,  $F=7.15$ ). Stiffness decrement beyond the elastic limit,  $k_{dec}$ , ( $p=0.003$ ,  $F=15.6$ ) and the elastic limit,  $x_e$ , ( $p < 0.001$ ,  $F=213.3$ ) both increased with velocity. Stiffness beyond the elastic limit,  $k_{after}$ , decreased with velocity. The elastic limit increased linearly with velocity from 0.025 to 0.065 rad, while the time to reach the elastic limit was surprisingly constant,  $x_t=29.5$  ( $\pm 0.8$ ) ms.

### 3.3. Effect of joint torque on short range stiffness

SRS increased with torque ( $p < 0.001$ ,  $F=123.2$ , Fig. 5) with averages of 15 Nm/rad for the lowest torque level to 23 Nm/rad for the highest torque level. Stiffness decrease beyond the elastic limit,  $k_{dec}$ , increased with torque ( $p < 0.001$ ,  $F=62.7$ ), although to a lesser extent as compared to SRS. The elastic limit decreased with torque ( $p=0.002$ ,  $F=9.95$ ).

### 3.4. The initial mechanical response

Joint torque (within the 40 ms time window) could be described by an inertial component, representing the wrist inertia, and an elastic component, representing the SRS from the wrist flexor muscles exclusively. The effect of joint damping  $b_j$  was negligible (see Section. 2.4). Fig. 6 shows the average simulated traces for inertia and elasticity over time for the extreme velocities (columns) and torque levels (bottom rows). The inertial torque (blue) dominates over the first 23 ms of the response and the elastic torque (red) thereafter. The decrease in the rate of elastic torque increment is clearly visible around 30 ms. The inertial torque increased with stretch velocity (higher acceleration) while the elastic torque increased both with velocity and voluntary torque. The black traces denote the summation of inertial and elastic joint torque, equal to the torque applied by the hand to the joint, i.e.  $T_h$  (Eq. (6)).

## 4. Discussion

Short range stiffness (SRS) parameters that were attributed to the cross-bridges and series elasticity from tendinous tissues were estimated from in vivo recordings of torque and angle of the wrist joint. The results showed that the velocity of imposed joint movement had strong effect on the elastic limit, i.e. the range over which the SRS was manifest, but not on SRS itself. It is concluded that the elastic limit of the wrist flexor muscles was determined by a constant time instead of being a length related property.

### 4.1. The elastic limit linearly increases with joint angular velocity

Joint elastic behavior appeared to be largely determined by the movement velocity because the elastic limit increased by a factor

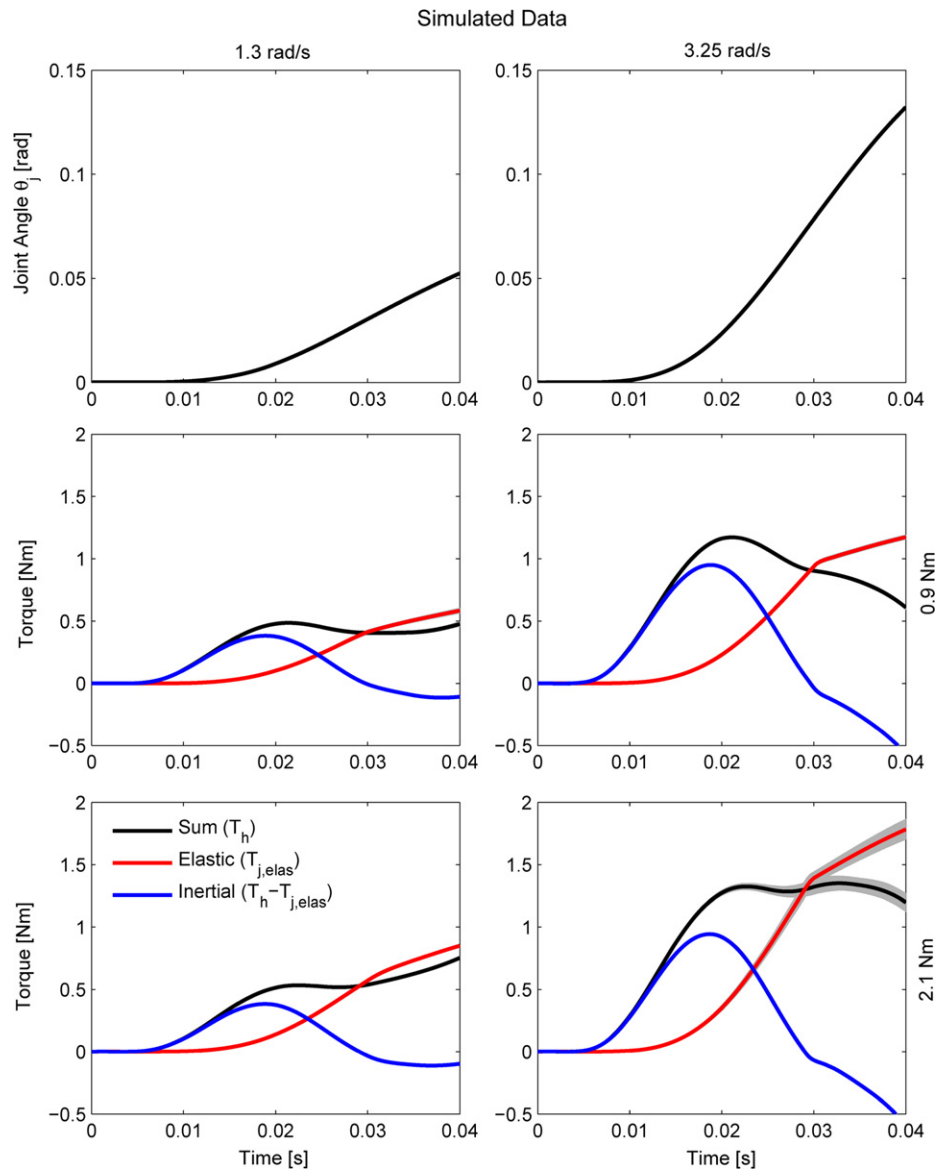


**Fig. 6.** Simulated data (solid: means; shading: 3 times standard deviation) for a typical subject at the smallest movement velocity (left column) and highest velocity (right column). Top row: wrist angle  $\theta_j$ , middle row: torque applied to the joint by the hand  $T_h$  (black), the elastic joint torque  $T_{j,elas}$  due to SRS (red) and the inertial joint torque being the difference between  $T_h$  and  $T_{j,elas}$  (blue), for the 0.9 Nm (middle row) and 2.1 Nm condition (bottom row), respectively. (For interpretation of the references to color in this figure legend, the reader is referred to the web version of this article.)

of 2.5 between the lowest and highest velocity applied (Fig. 5). For comparison of the results to previous findings on single muscles and fibers, the elastic limit was expressed as relative muscle strain. For this purpose, we used the relationship provided (van Eesbeek et al., 2010): 0.066 rad wrist rotation corresponding to  $17 \pm 4$  nm stretch per half sarcomere for the wrist flexor muscles. Using  $L_0 = 2.8 \mu\text{m}$  as the sarcomere length at neutral wrist angle (Friden and Lieber, 2002), 0.066 rad wrist rotation results in a mean strain of  $34/2800 = 1.2\%L_0$ . Applied to the current results (Fig. 5), the elastic limit varied between 0.5 and  $1.2\%L_0$ . As the elastic limit was reached in 30 ms, the corresponding relative velocities varied between 17 and  $40\%L_0/s$ . For comparable velocities, Campbell and Lakie (1998) found the elastic limit to range from 0.3 to  $0.4\%L_0$  (although slightly less than proportional with velocity) for relaxed frog muscle, while Rack and Westbury (1974) found values ranging from 1.4 to  $2.5\%L_0$  for active muscles of the cat. Our values were in between these ranges, which can be explained from differences in sarcomere

length amongst different vertebrates (Burkholder and Lieber, 2001), altered cross-bridge kinetics in the relaxed state (Hill, 1968; Lakie et al., 1984) and overestimation of muscle stretch due to strain of tendinous tissue for larger levels of activation (Cui et al., 2007; Rack and Westbury, 1974). The velocity dependency of the elastic limit was attributed to detachment of cross-bridges in such a way that cross-bridges during a rapid movement would probably move further before being broken down than it would in a slow movement (Rack and Westbury, 1974).

A linear increase of the elastic limit with movement velocity implicated a constant SRS period of about 30 ms (Fig. 5). We did not find any studies that explicitly reported on SRS period. However, from inspection by eye and at comparable velocities, an SRS period of 50 ms was derived from Rack and Westbury (1974). In contrast, the results from Campbell and Lakie (1998) clearly indicated a decrease in SRS period of about 50 ms, for much slower velocities than used here, to 5 ms for much higher velocities. If the 'true' SRS period, or elastic limit, would indeed be

nonlinearly related to stretch velocity, then the range of velocities used here likely covered a rather constant portion of these characteristics. Our results suggest that cross-bridges that were attached prior to the imposed stretch remain attached for approximately 30 ms for the applied range of velocities and torques.

#### 4.2. Short range stiffness did not change with angular velocity

No significant changes of wrist joint SRS with angular velocity were observed in this study. Invariant SRS with stretch velocity was also reported for the cat soleus and lateral gastrocnemius muscles but under stretch velocities that conditionally were ‘not too slow’ (Rack and Westbury, 1974). In relaxed frog muscle fibers at 5.5 °C both SRS and elastic limit force (i.e. the force at the elastic limit) increased less than proportional with lengthening velocity (Campbell and Lakie, 1998). Apart from differences in cross-bridge kinetics between relaxed and active fibers (Hill, 1968) and the effect of temperature on the elastic limit force (Flitney and Hirst, 1978), we can assume that muscle stretches in our study were fast enough not exhibiting any significant effect on SRS from stretch velocity. Apparently, the velocity of muscle stretch did not significantly change the average number of attached cross-bridges during elongation.

#### 4.3. Force decay beyond the elastic limit

Viscosity for the muscle–tendon part was found to be negligible with respect to its stiffness (joint damping  $b_j=10^{-5}$ ) and only seemed to appear in our model to prevent numerical instability. Hence, the predicted response of the wrist was inertial–elastic (Fig. 6) up to the elastic limit. The stiffness beyond the elastic limit  $k_{after}$ , i.e. the slope of the force length relationship, decreased with stretch velocity (Figs. 5 and 6). A similar observation was reported by Flitney and Hirst (1978) from active frog muscles. It seems likely that  $k_{after}$  represented a reduced resistance from cross-bridges that just loosened and re-attached at a shorter bonding length and that for faster stretches there would be insufficient time for re-attachment to occur (Flitney and Hirst, 1978; Sugi, 1972).

#### 4.4. Functional implication

The increase of elastic limit with velocity and related breakage (loss of strain energy) of cross-bridges beyond the elastic limit implicates that the amount of work dissipated by the joint also increases with velocity, e.g. compare the areas under the elastic torque–angle curves in Fig. 6. For impact situations where deceleration of the limb is important, the amount of kinetic energy that needs to be absorbed increases with velocity and requires concomitant dissipating capacity of the joint. This only holds for the initial stretch, whereas energy dissipation after the elastic limit relatively decreases.

#### 4.5. Future research

In many muscular and neurological diseases like inclusion body myositis (IBM), Stroke and Cerebral Palsy, a discrepancy is observed between the paresis, i.e. the net joint torque, and the clinical joint stiffness, observed as resistance against movement (Dietz and Sinkjaer, 2007). The current SRS measurement method can potentially be used to discriminate the contribution of active muscle from connective tissue even before reflexive torque is observed. Objective and quantitative discrimination between these passive, active and reflexive components is essential for targeted treatment.

On the muscle fiber level the time course of the force during small amplitude shortening was found to be opposite to the same amount of lengthening, suggesting a symmetric mechanical

response of cross-bridges with movement direction (Roots et al., 2007). Whether such a symmetric behavior in SRS is also manifest on the joint level remains to be studied and is relevant for understanding joint resistance during alternating displacements. Currently we apply our method to concentric loading.

## 5. Conclusion

We found that the velocity of rotation linearly increased the distance over which the joint behaved elastic. This, so called, elastic limit marks the transition from primarily elastic to primarily viscous behavior of the muscle–tendon unit. These findings correspond well to previous animal studies and most likely reflect the number of cross-bridges that are attached (before the elastic limit) and resumed to turn-over (beyond the elastic limit). The fact that the results of the present human in vivo study are in concordance with previous reports from single muscles and fibers in animal studies strongly supports our claim that cross-bridge properties can be quantified in vivo at the integrated joint level. We expect this technique to be important for clinical purposes, in particular for muscular diseases where the contractile machinery is affected.

## Conflict of interest statement

The authors declare that there is no conflict of interest that could influence the scientific content of the presented work.

## Acknowledgment

This work was part of the ROBIN project (ROBot-aided system Identification: novel tools for diagnosis and assessment in Neurological rehabilitation), supported by a grant from the Dutch Technology Foundation (STW), grant number 10733.

## References

- Axelsson, H.W., Hagbarth, K.E., 2001. Human motor control consequences of thixotropic changes in muscular short-range stiffness. *J. Physiol.* 535, 279–288.
- Burkholder, T.J., Lieber, R.L., 2001. Sarcomere length operating range of vertebrate muscles during movement. *J. Exp. Biol.* 204, 1529–1536.
- Campbell, K.S., Lakie, M., 1998. A cross-bridge mechanism can explain the thixotropic short-range elastic component of relaxed frog skeletal muscle. *J. Physiol.* 510 (Pt 3), 941–962.
- Cui, L., Perreault, E.J., Sandercock, T.G., 2007. Motor unit composition has little effect on the short-range stiffness of feline medial gastrocnemius muscle. *J. Appl. Physiol.* 103, 796–802.
- Dietz, V., Sinkjaer, T., 2007. Spastic movement disorder: impaired reflex function and altered muscle mechanics. *Lancet Neurol.* 6, 725–733.
- Flitney, F.W., Hirst, D.G., 1978. Cross-bridge detachment and sarcomere ‘give’ during stretch of active frog’s muscle. *J. Physiol.* 276, 449–465.
- Friden, J., Lieber, R.L., 2002. Mechanical considerations in the design of surgical reconstructive procedures. *J. Biomech.* 35, 1039–1045.
- Grillner, S., 1972. The role of muscle stiffness in meeting the changing postural and locomotor requirements for force development by the ankle extensors. *Acta Physiol. Scand.* 86, 92–108.
- Hill, D.K., 1968. Tension due to interaction between the sliding filaments in resting striated muscle. The effect of stimulation. *J. Physiol.* 199, 637–684.
- Kirsch, R.F., Boskov, D., Rymer, W.Z., 1994. Muscle stiffness during transient and continuous movements of cat muscle: perturbation characteristics and physiological relevance. *IEEE Trans. Biomed. Eng.* 41, 758–770.
- Lakie, M., Walsh, E.G., Wright, G.W., 1984. Resonance at the wrist demonstrated by the use of a torque motor: an instrumental analysis of muscle tone in man. *J. Physiol.* 353, 265–285.
- Lin, D.C., Rymer, W.Z., 1993. Mechanical properties of cat soleus muscle elicited by sequential ramp stretches: implications for control of muscle. *J. Neurophysiol.* 70, 997–1008.
- Loram, I.D., Maganaris, C.N., Lakie, M., 2007. The passive, human calf muscles in relation to standing: the non-linear decrease from short range to long range stiffness. *J. Physiol.* 584, 661–675.

- Morgan, D.L., 1977. Separation of active and passive components of short-range stiffness of muscle. *Am. J. Physiol.* 232, C45–C49.
- Rack, P.M., Westbury, D.R., 1974. The short range stiffness of active mammalian muscle and its effect on mechanical properties. *J Physiol* 240, 331–350.
- Roots, H., Offer, G.W., Ranatunga, K.W., 2007. Comparison of the tension responses to ramp shortening and lengthening in intact mammalian muscle fibres: crossbridge and non-crossbridge contributions. *J. Muscle Res. Cell Motil.* 28, 123–139.
- Sugi, H., 1972. Tension changes during and after stretch in frog muscle fibres. *J. Physiol.* 225, 237–253.
- van Eesbeek, S., de Groot, J.H., van der Helm, F.C., de Vlugt, E., 2010. In vivo estimation of the short-range stiffness of cross-bridges from joint rotation. *J. Biomech.* 43, 2539–2547.
- Walmsley, B., Proske, U., 1981. Comparison of stiffness of soleus and medial gastrocnemius muscles in cats. *J. Neurophysiol.* 46, 250–259.